

Use of Profilometry-Based Indentation Plastometry to Study the Effects of Pipe Wall Flattening on Tensile Stress–Strain Curves of Steels

Marcus Warwick, Harika Vaka, Chizhou Fang, Jimmy Campbell, James Dean, and Trevor William Clyne*

Herein, the flattening and subsequent tensile testing (in the hoop direction) of steel pipes used for transmission of oil and gas are concerned. A particular focus is on the use of a novel indentation plastometry test (PIP), applied to the outer free surface of an as-received pipe. This allows a stress–strain curve to be obtained from a relatively small volume (a disk of diameter about 1 mm and thickness around 100–200 μm). Whole section and reduced section tensile testing, of as-received and flattened samples are carried out. Four different pipes are studied. While there are some variations between them, there is a general trend for near-surface regions of the pipe to be a little harder than the interior, and for flattened pipes to be a little harder than unflattened ones, although these are not dramatic or well-defined effects. PIP testing also confirms that these pipes exhibit little or no anisotropy. It is in general concluded that PIP-derived stress–strain curves for testing of the outside of a pipe are likely to be quite close to those obtained by tensile testing of the whole section in the hoop direction, after flattening.

1. Introduction

An important issue within the mechanics of materials is that of how (differential) prior plastic deformation affects the stress–strain relationship subsequently exhibited by metallic components. For example, rolling of sheet or plate tends to create higher plastic strains in the near-surface layers, which in general tends to harden those regions. This will create inhomogeneity in the product, but other effects may also arise. These include an anisotropic response to subsequent loading and the creation

of residual stresses within the sheet. The length scale over which such variations are created is often too fine for their study via conventional uniaxial testing. This is partly a practical issue arising from the difficulty of obtaining very small tensile samples, although there are also theoretical problems, in the sense that unconstrained samples with very small ($\approx < 1$ mm) lateral dimensions may behave differently from the bulk.^[1]


However, the recently developed testing procedure of profilometry-based indentation plastometry (PIP) has the potential for obtaining stress–strain relationships from regions with dimensions of the order of a mm, without the sample itself being small. Moreover, it also reveals information about any (in-plane) anisotropy exhibited by the region concerned. It is built on

extensive prior work covering various aspects of the use of an indentation outcome to infer the stress–strain relationship of the sample material. Some of this work is summarized in recent papers.^[2–5] Specific details of the PIP procedure are described in several recent papers,^[6–11] one of which is focused on the study of anisotropic samples.^[9] There is therefore scope for using this testing methodology to study how prior differential plastic straining has affected the local response of a metallic component. This can then be compared with outcomes of conventional (larger scale) testing procedures. A particular focus for this is provided by the case of a section of steel pipe having its curvature in the transverse plane reduced to zero (“flattening”) by plastic straining, before being tensile tested in what was originally the hoop direction. This response is of particular interest, since it is in this direction that the peak stress is generated by internal pressurization under service conditions. There are, of course, difficulties in carrying out conventional tensile testing in the hoop direction of a pipe, unless its diameter is very large.

Such testing of flattened samples is common in commercial practice. Several papers^[12–15] report on effects of the flattening, with it being widely reported that significant changes can be induced by the operation. Most such publications simply report these changes, which often take the form of reduction in yield stress being caused by the flattening. Kang et al.^[14] also found that on tensile testing thin samples from different locations within the wall section, the reduction was greater on the side that

M. Warwick, H. Vaka, C. Fang, J. Campbell, J. Dean, T. W. Clyne
204 Science Park
Milton Road, Cambridge CB4 0GZ, UK
E-mail: twc10@cam.ac.uk

T. W. Clyne
Department of Materials Science
University of Cambridge
27 Charles Babbage Road, Cambridge CB3 0FS, UK

 The ORCID identification number(s) for the author(s) of this article can be found under <https://doi.org/10.1002/srin.202200920>.

© 2023 The Authors. Steel Research International published by Wiley-VCH GmbH. This is an open access article under the terms of the Creative Commons Attribution License, which permits use, distribution and reproduction in any medium, provided the original work is properly cited.

DOI: 10.1002/srin.202200920

was strained in compression. They attribute this to a Bauschinger effect. It is also sometimes reported^[15] that there is greater variability with flattened samples. One of the problems here is that much of the work in this area is reported only in the form of values for the yield stress (YS), and perhaps the ultimate tensile stress (UTS), with the full stress–strain curves not being provided. This constitutes a limitation, since the full curve is often more informative (and values of the YS may vary, depending on exactly how it is derived from the curve). Detailed explanations of the observed effects are usually lacking, although it is often recognized that prior plastic deformation is in general likely to cause hardening. At first glance, therefore, it is surprising that a fall in the YS is often reported, although it's certainly possible that there could be a Bauschinger effect, such that a lower tensile YS might be expected on the side (the “outside”) that was subjected to prior compressive strain in the loading direction. Some effort has been directed toward standardization of the flattening procedure.^[12,13] There have also been suggestions^[14] about how the flattening should be done in order to minimize strain localization during the process. However, this still leaves the observed effects largely unexplained and there are no guidelines for taking them into account in any systematic way (other than purely empirical correlations).

In fact, the main effects that are theoretically expected to arise during flattening can readily be identified. If springback is neglected, and in practice it is often observed to be small, then the change in curvature during flattening will be given by $1/R$, where R is the radius of the pipe (distance from pipe axis to mid-plane of the wall). The plastic strain induced by this flattening, at a distance γ from the neutral axis (mid-plane), is simply γ/R . For example, with a pipe radius of 100 mm and a wall thickness of 10 mm, the peak plastic strain (at the two free surfaces) in a flattened section will be $\pm 5\%$. This strain will be in the hoop direction (with plastic strains in axial and/or radial directions occurring to conserve volume). These are not huge strains, even for this case of a relatively thick wall (for this pipe radius). Nevertheless, depending on the work hardening characteristics, they could induce significant changes in the local yielding and plasticity response. Furthermore, the fact that the properties may now vary with location in the cross section of the tensile test piece, and that there may also be residual stresses in the sample, could affect the measured stress–strain curve.

It should, of course, be recognized that, from a mechanistic point of view, the effect of prior plastic deformation on the subsequent response is potentially highly complex. It will in general involve local changes in dislocation density, crystallographic texture, grain boundary structures, distribution of precipitates and solute atoms, etc. However, there is little or no scope for using such information to predict the mechanical response. There is no real alternative to ascribing a true (von Mises) stress–true (von Mises) plastic strain relationship to the material (treated as a continuum), obtained on a purely empirical (experimental) basis. For an isotropic, homogeneous material, the obtaining and implementation of such a relationship is straightforward and can be used, for example, in finite-element method (FEM) simulation of a particular type of deformation process or testing procedure. It is, in fact, also possible^[16–18] to carry out such a procedure when the material is inhomogeneous and/or anisotropic, provided the necessary input data are available.

Regarding the potential use of indentation testing to obtain information about material response on a local scale, it is sometimes claimed that “nanoindenters” can be used to infer stress–strain relationships, with fine-scale resolution. However, a key finding from detailed study over recent years^[6] is that the plastically deformed volume must be large enough for its mechanical response to be representative of the bulk. This usually requires it to be a “many-grained” assembly, which typically translates into a need for the indenter radius to be of the order of 0.5–1 mm and the load capability to extend to the kN range. This means that nanoindenters (typically having maximum loads of a few tens of Newtons at most) are completely unsuitable. There have, however, been a number of investigations based on use of relatively large (spherical) indenters, including a few,^[19] in which anisotropy was investigated. In particular, the PIP procedure has been used^[9] to study both anisotropy and inhomogeneity in additively manufactured materials. It has been shown to have a high sensitivity for detection of (plastic) anisotropy via a lack of radial symmetry in the indent, with greater pile-up heights in softer (in-plane) directions. It is employed here as part of an investigation into the details of how the flattening of steel pipes can affect the measured tensile stress–strain curve of the material.

2. Experimental Section

2.1. Materials and Pipe Geometries

This paper covers data acquired from 4 pipes, each having a different composition and pipe geometry, before and after a flattening operation (removal of the curvature from a section of pipe). They all had approximately the same diameter (260–270 mm ≈ 10 inches), but with a range of wall thickness (5–9 mm). No information is available about the conditions under which the pipes were produced, but they were all seamless pipes made by the rotary mandrel piercing (Mannesmann) process.^[20,21] The exact compositions of the four steels were unknown. They were, however, all plain carbon steels and their stress–strain curves (see below) were all different, so it's likely that there were certain differences (in carbon content and possibly in the level of elements such as Mn and Si). Their microstructures, which were primarily ferritic, with some pearlite, were all fairly similar. **Table 1** gives the pipe dimensions, with a code letter for each of the steels. Also shown is the ratio of wall thickness to diameter, which represents the peak plastic strain created in the pipe (along the hoop direction) when it is flattened. These pipes were thought to represent a cross section of those used commercially for long-distance transmission of oil and gas.

Table 1. Pipe codes, with corresponding dimensions.

Pipe Code	Steel	Dimensions [mm]		Peak Plastic Strain from Flattening [%]
		Radius, R	Wall thickness, $2h$	
P1	A	135	5	1.9
P2	B	135	9	3.3
P3	C	135	8	2.9
P4	D	130	5.5	2.1

2.2. Flattening Procedure

Pipes were flattened by compressing a section (an annular ring sector) between two hard platens. These sections had a chord length of about 80 mm, such that the “gap” between the lower platen and the inner concave surface of the pipe was about 6 mm. A load was progressively applied until this gap was closed and then raised a little above this level. The change in geometry during flattening is depicted schematically in **Figure 1**. This type of procedure is representative of those used commercially for this purpose, although it should be recognized that it is not very well defined. In general, the resulting plate was macroscopically flat, at least to a good approximation, that is, there was usually little or no “springback”.

2.3. Tensile Testing

Tensile testing was carried out using an Instron 3369, with a 50 kN capacity. Samples were rectangular in section, with the reduced section part having a width of 6 mm, a thickness in the range of 1–2 mm, and a length of 30 mm. These samples were produced by mechanical machining from appropriate sections of the pipe concerned. The clip gauge was 25 mm long. The nomenclature used for these tests is depicted in **Figure 1**. For example, in the designation T/A/z/4/1, the T refers to a tensile test, A means as-received (rather than flattened, F) and the z indicates that the loading axis is along the z direction (axis of the pipe). The value of 4 in this example gives the distance (in mm) between the neutral plane (midpoint) of the pipe and the center of the section being tested, while the value of 1 gives the thickness of the sample in the radial direction. (For whole section testing, the latter will be 2 h, while the former will be zero).

The (nominal) stress–strain curves presented here—including those derived from PIP testing (§2.4)—were curtailed at the onset of necking (peak in the plot, although it’s often a rather flat curve). None of these tensile tests involved fracture before this point. This was done because the postnecking parts of such curves had no universal significance (being dependent on the dimensions and geometry of the test-piece).

2.4. Indentation Plastometry (PIP Testing)

The PIP setup used in this work has been described previously.^[10] The procedure involved 1) pushing a hard spherical indenter into the sample with a known force, 2) measuring the (radially symmetric) profile of the resultant indent, and 3) iterative FEM simulation of the test to find the best fit set of plasticity parameter values in the Voce law.

$$\sigma = \sigma_s - (\sigma_s - \sigma_Y)e^{-\epsilon/\epsilon_0} \quad (1)$$

in which σ_Y is the yield stress, σ_s is a “saturation” level, and ϵ_0 is a characteristic strain for the exponential approach of the stress toward this level. The balls used were of Si_3N_4 , with a radius of either 1 mm (for as-received material) or 0.5 mm (for flattened material). The indent topographies were characterized with a stylus profilometer (resolution $\approx 1 \mu\text{m}$). The elastic constants of the material were provided as input parameters, in this case a Young’s modulus of 200 GPa and a Poisson ratio of 0.33. Various details were provided in a recent review paper.^[6] Recent publications also cover certain specific aspects, including effects of anisotropy,^[9] porosity,^[22] tensile-compressive asymmetry,^[23] residual stresses,^[8] and inhomogeneity.^[10]

The geometry of the PIP testing is also depicted in **Figure 1**. A designation such as PIP/F/r/3 refers to a PIP test on a flattened pipe, with the centerline of the indentation along r (radial, or through-thickness, direction). The value of 3 here indicates that the plane being tested is 3 mm away from the neutral plane of the pipe. This could be the original free surface of the pipe (in which case the value will be equal to h, the semithickness). Furthermore, while the tensile testing was done in z (axial) and θ (hoop) directions, PIP testing was carried out with the indentation centerline along all three principal directions (axial, hoop, and radial). PIP tests in axial and hoop directions were carried out on mounted pieces of complete pipe sections. Finally, when presenting an indent profile, it’s sometimes necessary to specify its (in-plane) direction (scan angle). For example, for a PIP/A/z/0 test, an extra parameter may be appended of 0° (hoop direction) or 90° (radial direction) or indeed potentially other scan angles as well.

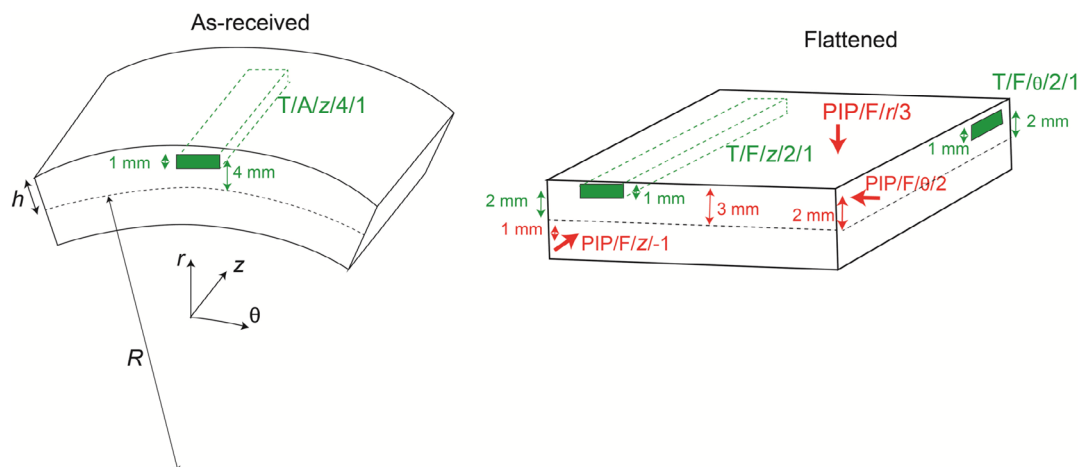


Figure 1. Geometry and nomenclature for pipe flattening and tensile or PIP testing.

2.5. Finite-Element Simulation of Flattening and Tensile Testing

In order to explore the expected effects of the pipe flattening operation, an FEM model was set up within COMSOL, reflecting the experimental arrangement. The geometry and dimensions are shown in **Figure 2**. There were 19 200 quadratic hexahedral elements in the pipe and 2500 linear hexahedral elements in the platens. An increasing load was applied to the upper platen, until the center of the pipe section touched the lower platen. The load was then removed. The “springback” after this had been done was relatively small, leaving the pipe section close to being flat. The distributions of residual stress and strain were investigated. Additionally, simulations were carried out of subsequent tensile testing operations, for both hoop and axial loading, with the whole of the section being tested.

3. Mechanical Test Outcomes

3.1. Tensile Testing of Undeformed and Flattened Pipe

The tensile stress–strain plots shown in **Figure 3** relate to P1, which is a relatively thin-walled pipe ($h/R \approx 1.9\%$), made of a fairly hard steel ($YS \approx 500$ MPa). This pipe is therefore one for which, in general, the effects of flattening would be expected to be relatively small. **Figure 3a** shows curves before and after the flattening operation, when tested across the complete thickness of the wall. These do indeed indicate that any changes are small—perhaps just a slight tendency for the yielding to become more transitional (gradual), giving a slightly lower yield stress (depending on how it is defined).

Figure 3b–d shows how the curves vary between the center and the near-surface regions of the wall. It may first be noted that the as-received pipe (**Figure 3b**) shows some variations, with

the center being softer in terms of YS (and the outer surface being a little harder than the inner surface). After flattening, the curves for axial and hoop directions (**Figure 3c,d**) are similar, which tends to be a general observation for most pipes. They both show that the central region is softer than the two near-surface regions. This is consistent with those regions both being plastically strained during the flattening, which is in general expected to cause some hardening, at least in terms of YS. While these strains are relatively low ($< \approx 2\%$), this is a steel that exhibits significant work hardening, so an effect of this type might be expected. It may also be noted that it’s not immediately clear how a set of curves like this will relate to a test that interrogates the complete section of the wall, partly because that may contain residual stresses that would be removed when machining small section testpieces from it.

Figure 4 relates to P2, which is a thicker-walled pipe ($h/R \approx 3.3\%$), made of a softer steel (compared with P1). The effects of flattening might thus be expected to be somewhat greater in this case. **Figure 4a** indicates that, when the complete wall thickness is tested, the flattening causes significant hardening, at least in terms of YS (rising from about 350 to 400 MPa for both axial and hoop testing). **Figure 4b–d** again indicates that these whole section tests are the outcomes of interrogating a volume that is far from homogeneous. **Figure 4b** again shows that the starting material is softer in the center than near the free surfaces. Furthermore, in this case, the flattening (**Figure 4c**) has accentuated this difference considerably, causing appreciable hardening of the near-surface regions (with YS values apparently rising to around 450–500 MPa). It may also be noted that the hardening is similar at the inner and outer surfaces. There is therefore no Bauschinger effect, since the outer surface underwent a compressive strain in the hoop direction, whereas the inner surface was subjected to a tensile strain in that direction.

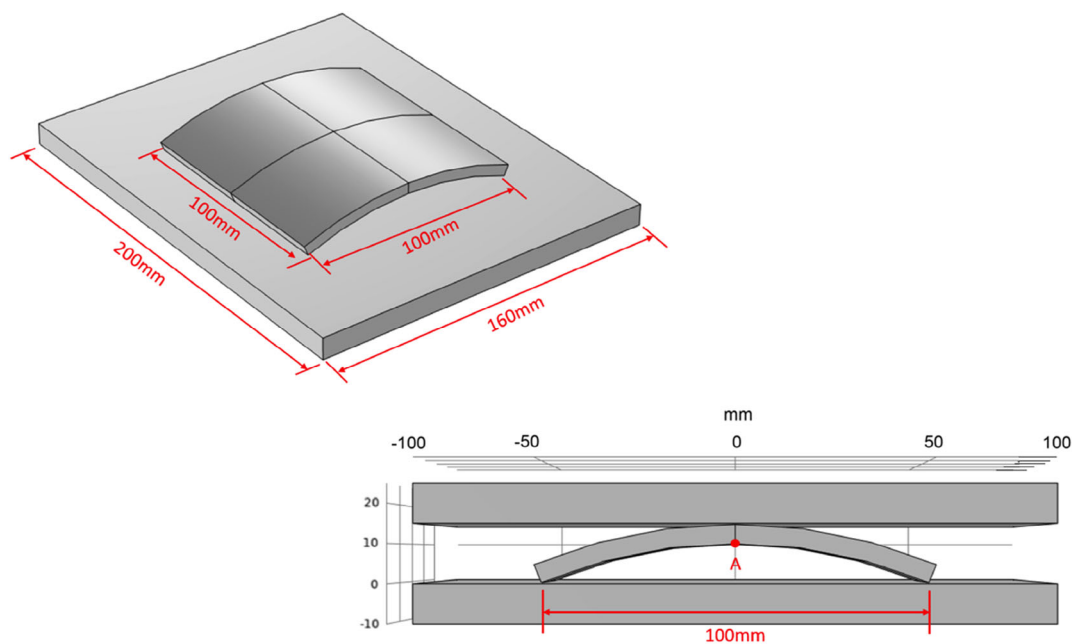


Figure 2. Perspective depictions of the FEM model geometry for flattening of a pipe with a diameter of 300 mm and a wall thickness of 6 mm. The flattening was carried out by applying a vertical force until point “A” touched the lower platen.

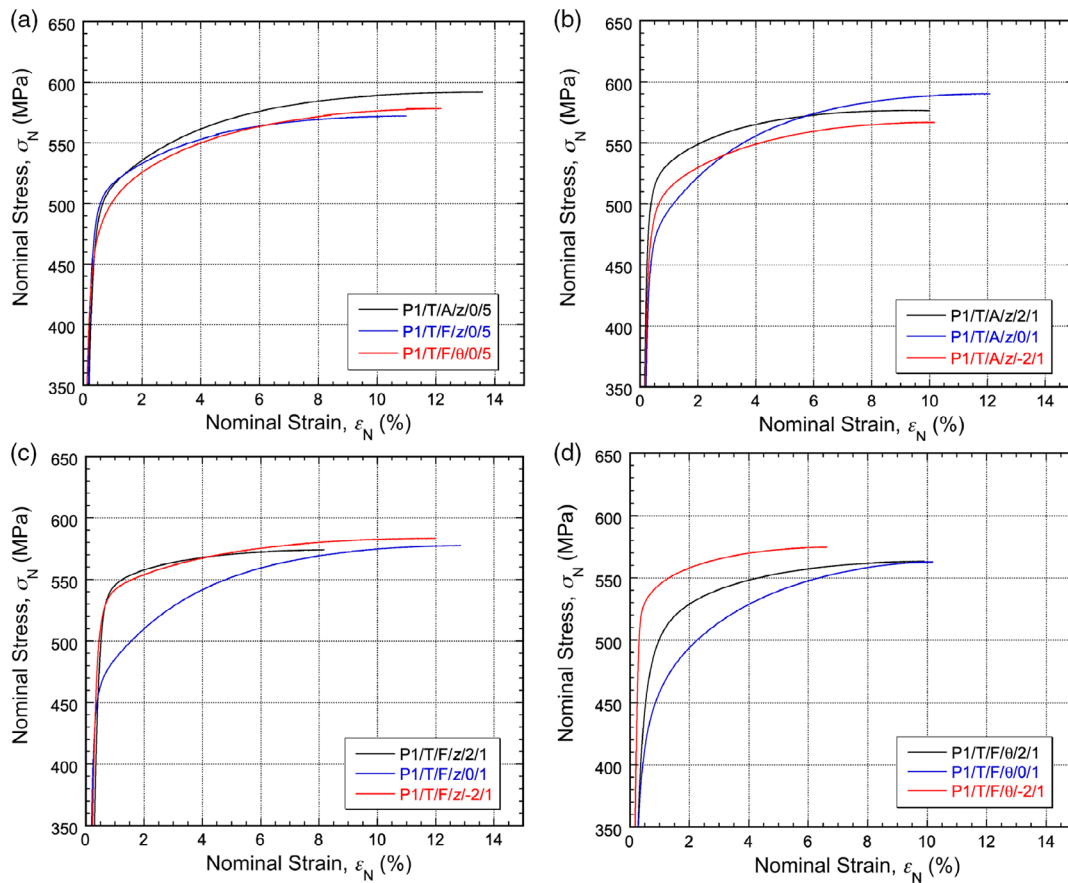


Figure 3. Nominal tensile stress–strain curves from pipe P1 for: a) complete through-thickness sections, before (axial) and after (axial and hoop) flattening, and localized section testing for b) axial as-received, c) axial flattened, and d) hoop flattened.

This is in fact a general observation and it seems likely that the flattening simply causes some strain hardening near the free surfaces, possibly with residual stresses also having an effect in some cases; see §4.

The plots shown in **Figure 5** are for a pipe (P3) with a fairly high ratio of wall thickness to diameter (2.9%), made of a steel that exhibits strain bursting (caused by escape of dislocations from carbon atmospheres and often associated with formation of Lüders bands in the sample). This effect tends to be noticeable only in steels with low carbon levels and without significant alloy additions. Such strain bursting—up to a level of around 2%—can be seen in the whole section test of the as-received pipe (**Figure 5a**), but it disappears after flattening. In addition, the flattening again causes some (limited) hardening. **Figure 5b** shows that the strain bursting is observed for all parts of the wall in the as-received pipe, with little or no variation between them. After flattening, on the other hand, some changes are induced between the responses from different locations, with some strain bursting retained in the center, but none seen in the outer regions. There is again some hardening of the near-surface regions, relative to the center.

This effect of flattening in removing the strain bursting in deformed regions is as expected, since it's well established that the effect tends to disappear after some initial straining, as

dislocations escape from their atmospheres. In fact, depending mostly on the temperature, these atmospheres might be expected to reform, although this could take quite a long time at ambient temperatures. In practice, the strain bursting often has relatively little effect on the overall plasticity, so it's not of critical importance that it should be captured during a test. The basic effect of the flattening is again some hardening of the near-surface regions.

Figure 6 illustrates that further complexities are possible in terms of the detailed response to flattening. These curves refer to a pipe (P4) with a relatively low h/R ratio (2.1%), which also tends to exhibit strain bursting and has a low YS (300 MPa). In fact, for testing of the whole section (**Figure 6a**), this strain bursting appears to be minimal, and the flattening apparently has little effect. However, **Figure 6b** reveals that, in the as-received pipe, the central region exhibits quite marked strain bursting, but there is none in the outer regions, which is also significantly harder. It seems likely, therefore, that the outer regions of this pipe were preferentially strained during its production. This is certainly possible, depending on the production method and the conditions employed (which are unknown for all these pipes). The flattening process has not actually changed these properties very much, with the strain bursting retained in the central region and the near-surface regions retaining their greater hardness.

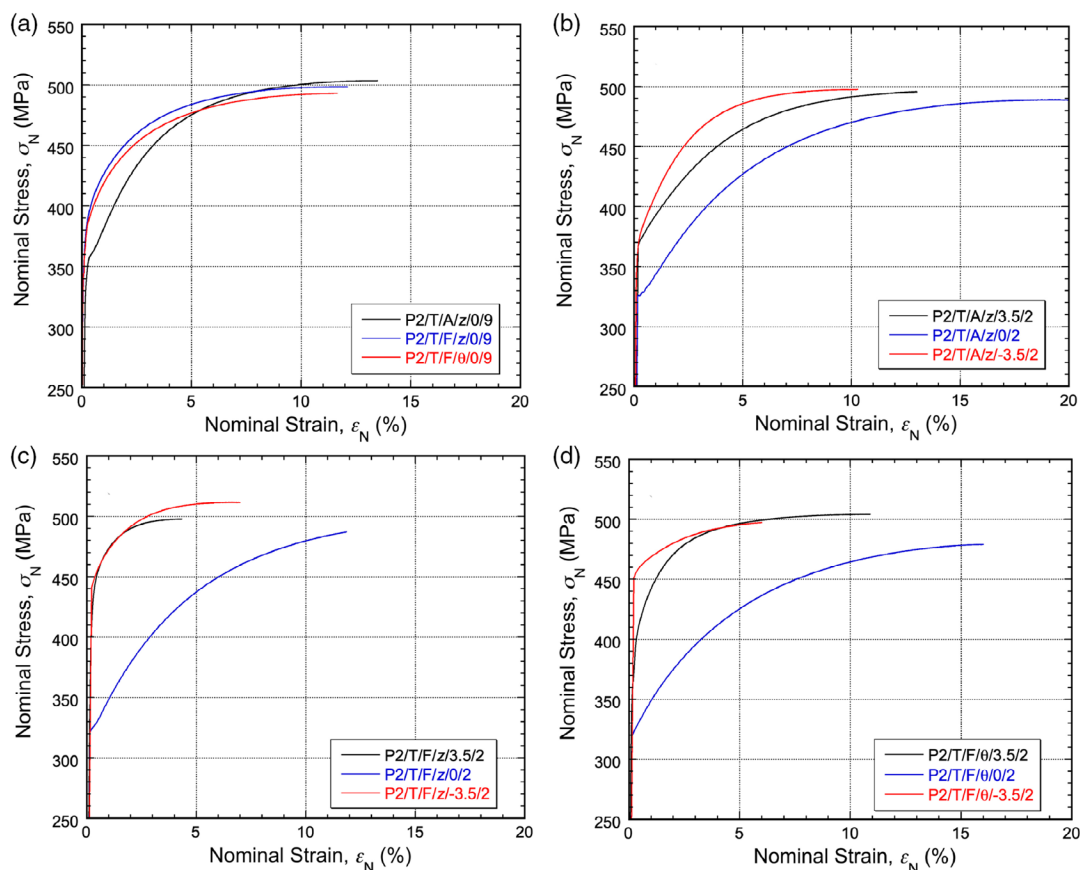


Figure 4. Nominal tensile stress–strain curves from pipe P2 for: a) complete through-thickness sections, before (axial) and after (axial and hoop) flattening, and localized section testing for b) axial as-received, c) axial flattened, and d) hoop flattened.

It would be difficult to have prior knowledge of this kind of effect when mechanically interrogating the outer region of a pipe, although the basic observation that it is expected to be harder than the interior is likely to be valid.

3.2. PIP Testing

3.2.1. Inferred Nominal Stress–Strain Curves

The experimental outcome of a PIP test is a set of indent profiles or, if the indent exhibits radial symmetry, a single profile (height as a function of radial distance from the indentation centerline). Such symmetry was observed for all of the indents made with the centerline in the radial direction. These profiles are converted (via iterative FEM modelling) to true stress–true plastic strain relationships, captured in the form of a set of three parameter values in the Voce constitutive law. These are then converted to nominal stress–nominal strain curves for uniaxial tensile testing, up to the onset of necking, using the standard analytical relationships. These are presented here for the same set of pipes as those in §3.1.

The PIP-derived stress–strain curves for pipe P1 are shown in **Figure 7**. Also included in these plots, for comparison, are corresponding tensile test outcomes (from **Figure 3b,c**). **Figure 7a** refers to the as-received pipe, while **Figure 7b** refers

to the flattened condition. The comparisons shown are with the tensile data for axial loading. Hoop loading tensile curves cannot be obtained for the as-received pipe, but those for the flattened pipe are similar to the corresponding ones for axial loading. This simplifies matters, since the PIP plots are expected to be an average of those for the two in-plane directions (axial and hoop). Accepting that the PIP and tensile tests don't refer to exactly the same locations (with the PIP tests interrogating a thinner slice than the tensile tests), the correspondence is good, with confirmation that the central region is a little softer than the near-surface regions, both before and after flattening.

Corresponding plots for pipe P2 are shown in **Figure 8**, again including comparison with the curves in **Figure 4b,c**. There is again good general consistency. This is a softer steel than for P1, but it has a higher initial work hardening rate and the outer regions are again harder than the center in the as-received condition. After flattening, this difference is accentuated slightly. **Figure 9** shows the data for pipe P3. There is again good consistency with the tensile plots. All three curves are similar in the as-received condition, with a YS around 300 MPa and UTS just below 500 MPa. After flattening, the near-surface regions have hardened a little. Of course, the strain bursting is not picked up by the PIP, but the overall curves are not strongly affected by this and in any event it largely disappears after flattening.

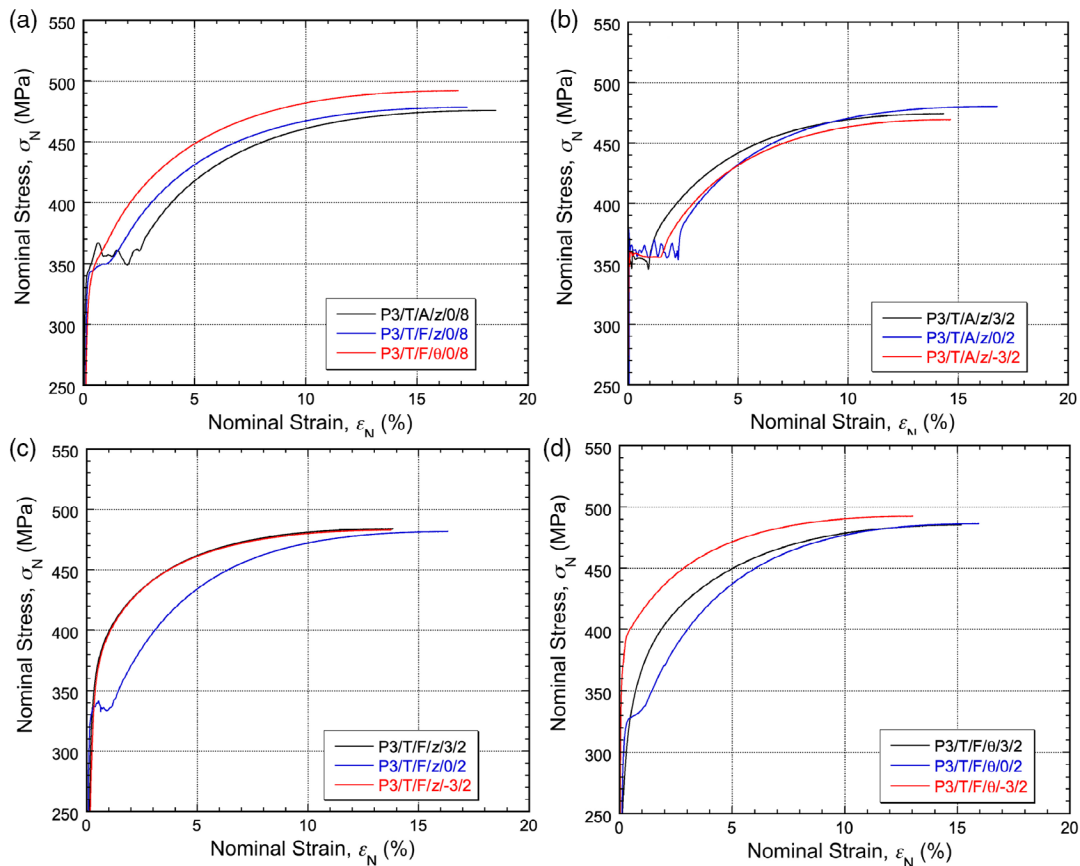


Figure 5. Nominal tensile stress–strain curves from pipe P3 for: a) complete through-thickness sections, before (axial) and after (axial and hoop) flattening, and localized section testing for b) axial as-received, c) axial flattened, and d) hoop flattened.

Finally, it can be seen in **Figure 10** that there is also good agreement for P4. In the as-received condition, the center is again a little softer than the near-surface regions. There is then some accentuation of this effect after flattening. Again, the strain bursting cannot be picked up by PIP, but again this has little effect on the overall curves. In summary, it's clear that the PIP testing is a reliable approach to obtaining stress–strain curves for these steels and to detecting any differences in response between near-surface and central regions.

3.2.2. Anisotropy

The PIP-derived stress–strain curves in **Figure 7–10** were all obtained by indenting with the centerline along the radial (through-thickness) direction. These indents were made into either the outer free surface (after some relatively coarse grinding) or into a relatively thick sample taken from the central region. In all cases, these indents were radially symmetric, at least to a very good approximation. This implies that there is no in-plane anisotropy, which is consistent with the fact that the tensile stress–strain curves are in all cases very similar for loading in hoop and axial directions (for flattened samples, hoop testing was not possible for as-received samples).

This still leaves the possibility of anisotropy in the through-thickness direction, relative to the in-plane directions. This is

not uncommon in components such as rolled plate, often with the through-thickness direction being somewhat softer. Such anisotropy is normally of little practical significance, but it is relevant to PIP, which is effectively testing the material in all directions. For these pipes, however, it was found that there was little or no such anisotropy. This can be seen from the profiles shown in **Figure 11**, which are from indents made in the z (axial) direction—that is, into the radial-hoop plane—near the mid-section, for all four pipes (in the as-received condition). The PIP procedure has high sensitivity for the detection of in-plane anisotropy, in the form of differences in pile-up height in different scan directions. For these pipes, however, such differences are very small, indicating that they are completely isotropic. This simplifies the relating of PIP-derived stress–strain curves to those obtained by tensile testing. For conversion of a PIP-derived curve, obtained by testing the outside of an as-received pipe, to one obtained by tensile testing a flattened sample in the hoop direction, only the effects of any inhomogeneity (differences between near-surface and interior properties), and of the flattening process itself, need to be taken into account.

3.2.3. Application of PIP to Field Testing of Pipes

A key objective of the current study is to relate the stress–strain curve obtained by indenting the outer surface of an as-received

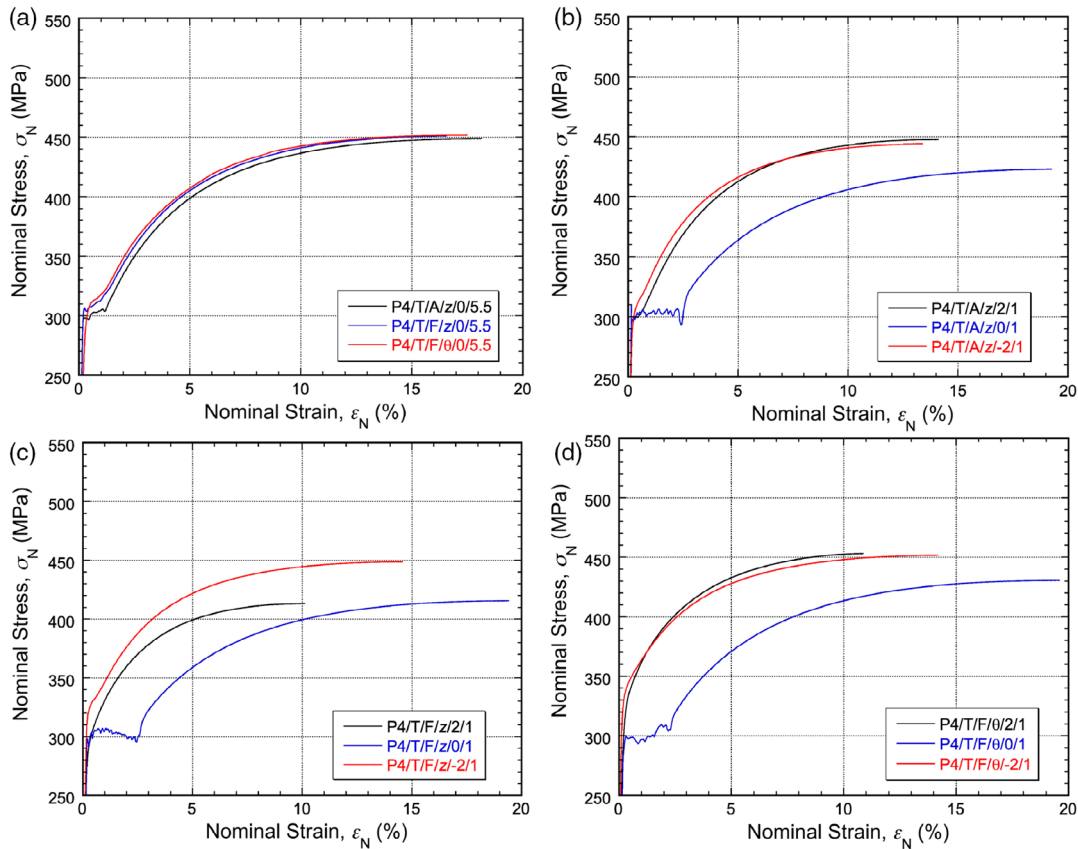


Figure 6. Nominal tensile stress–strain curves from pipe P4 for: a) complete through-thickness sections, before (axial) and after (axial and hoop) flattening, and localized section testing for b) axial as-received, c) axial flattened, and d) hoop flattened.

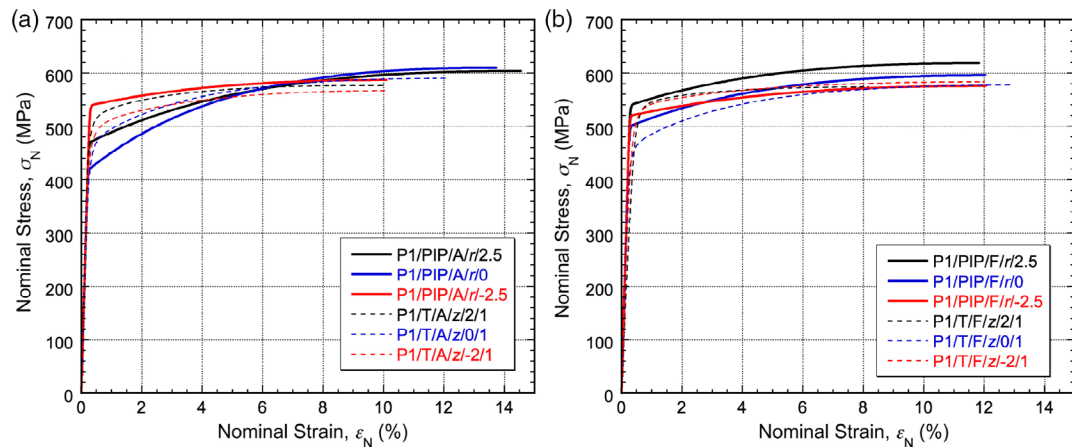


Figure 7. Nominal tensile stress–strain curves, obtained via PIP testing, with a centerline in the radial direction of pipe P1, at three different distances from the neutral plane for: a) as-received and b) flattened conditions. Also shown are corresponding tensile test curves, for axial loading.

pipe to the one that would be obtained by tensile testing (in the hoop direction, usually across the complete wall thickness) a flattened sample. The former is in fact likely to be the average of the curves in the hoop, axial, and radial directions. However, as noted above, these pipes tend to be at least approximately isotropic. PIP-derived stress–strain curves, obtained by field testing, will therefore be the solid black ones in

Figure 7a, 8a, 9a, and 10a. The target tensile test outcomes, on the other hand, will be the red curves in Figure 3a, 4a, 5a, and 6a.

A comparison is shown in **Figure 12** between these pairs of curves. They are in general quite close to each other. For pipes P2 and P3, a small “correction” might be needed in the form of the PIP result being “hardened” slightly, at least for the YS,

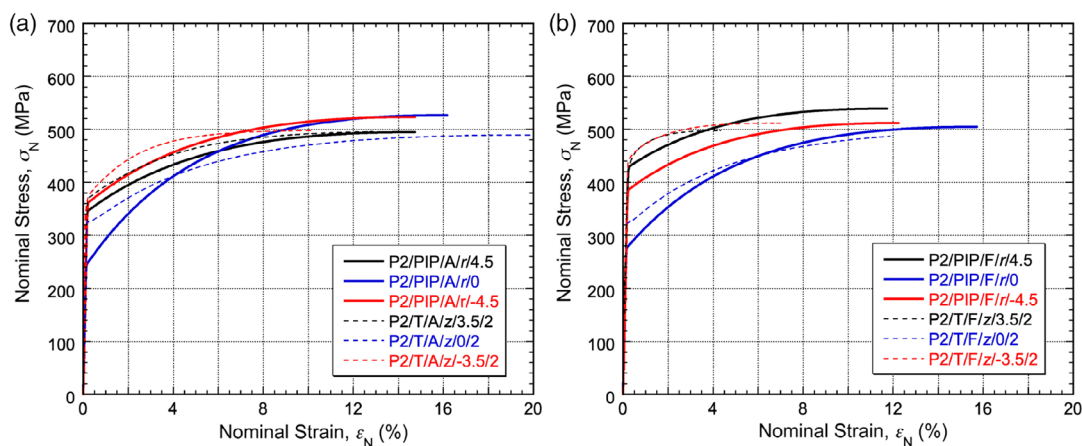


Figure 8. Corresponding comparisons to those of Figure 7, for pipe P2. a) as-received and b) flattened conditions.

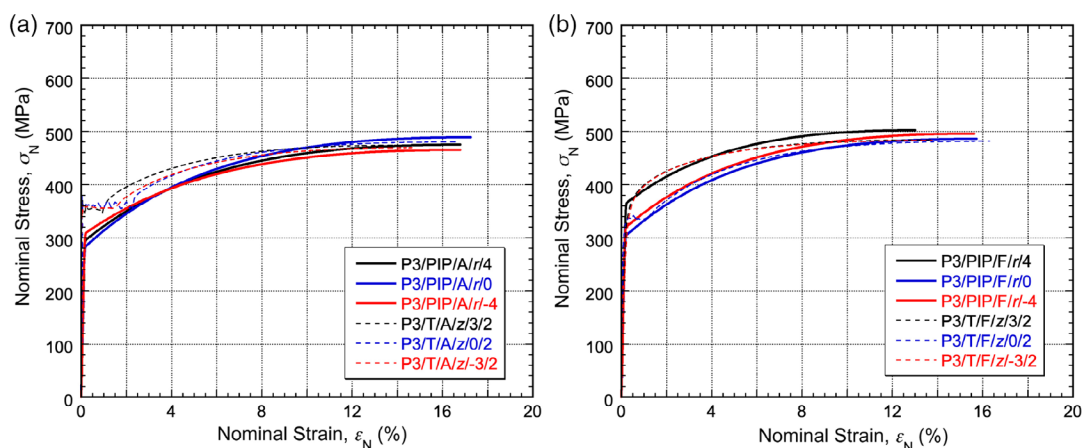


Figure 9. Corresponding comparisons to those of Figure 7, for pipe P3. a) as-received and b) flattened conditions.

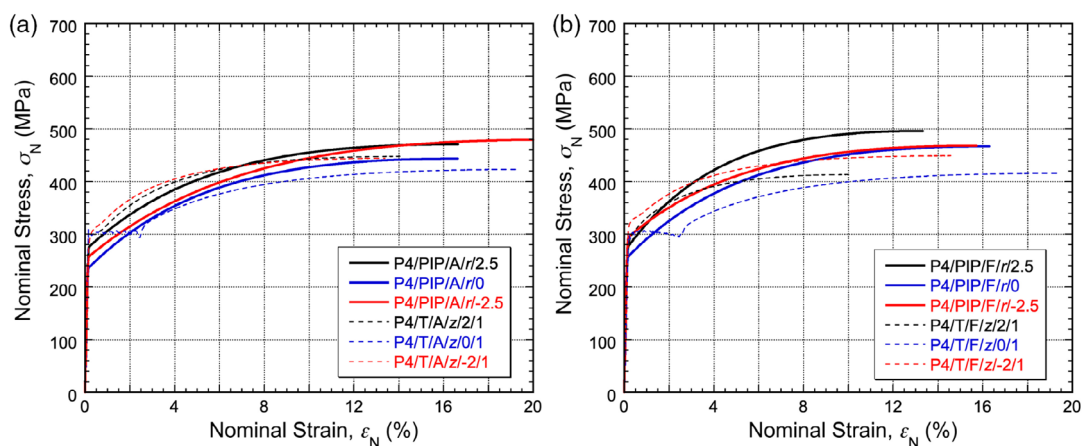


Figure 10. Corresponding comparisons to those of Figure 7, for pipe P4. a) as-received and b) flattened conditions.

whereas the other two would need little or no change. There is clearly an issue relating to exactly how the YS is defined and the likelihood that the tensile curve may exhibit transitional yielding, perhaps as a consequence of the flattening; see §4. For example, the PIP-inferred YS values for P2 and P3 (≈ 350 and 300 MPa

respectively) correspond quite closely with the onset of plasticity during the tensile test, but the actual YS values extracted from such tests, for example, using a 0.2% offset or 0.5% total strain construction, might be higher than these values by about 50 MPa. The overall shapes of these curves should be considered

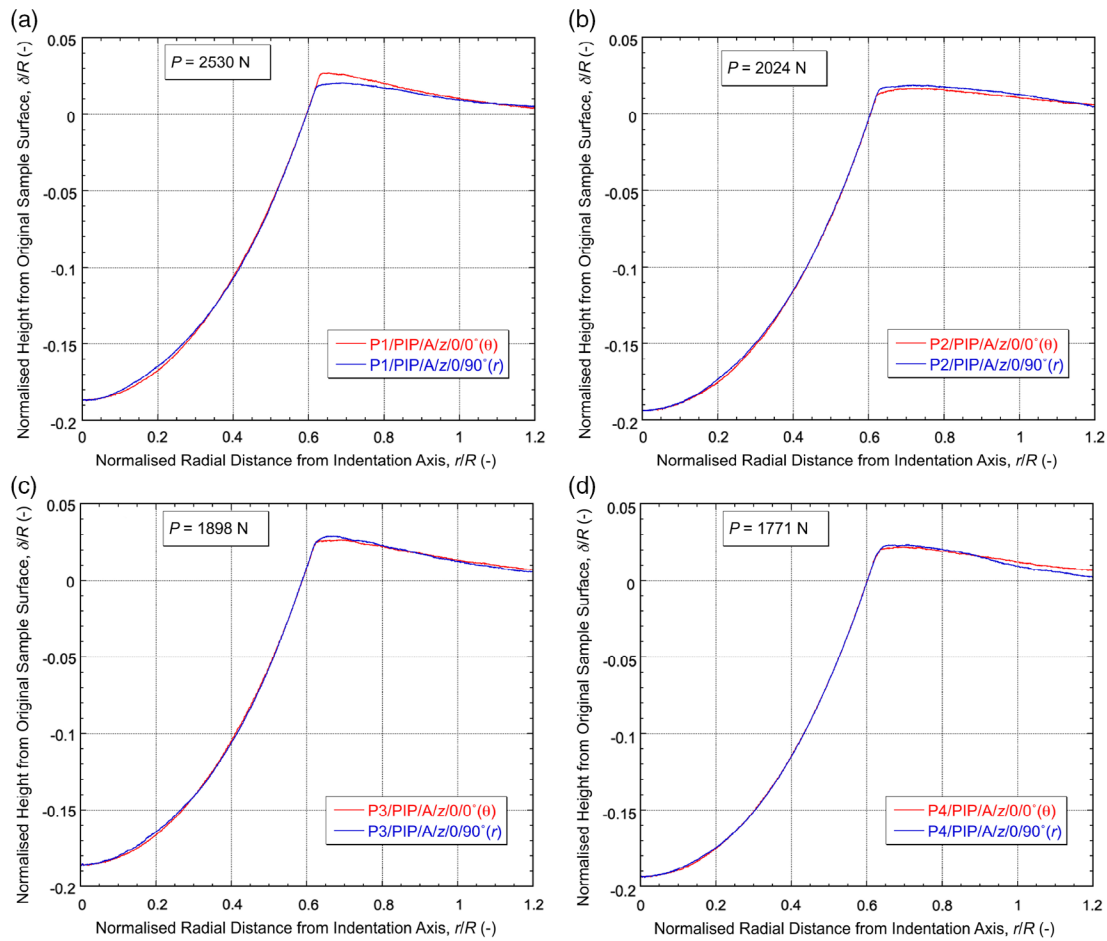


Figure 11. Measured indent profiles in 0° (hoop) and 90° (radial) directions, after indentation along the axial direction, near the midplane of the wall section, for the following pipes, all in the as-received condition: a) P1, b) P2, c) P3, and c) P4.

when making such comparisons (recognizing that the PIP procedure is insensitive to the yielding having a transitional nature).

The details are likely to depend on the h/R ratio of the pipe, as well as on the steel itself and on the way that the pipe was manufactured. However, in general, it seems unlikely that large corrections will be necessary. There may be an element of the outer surfaces of an as-received pipe being a little harder than the interior, while testing of the whole section of a flattened pipe gives an outcome that is a little harder than in the as-received condition. These two effects might to some extent cancel out when relating the outcome of an outer surface PIP test to the corresponding (flattened) tensile test result. Needless to say, some sort of error band will be appropriate for both types of tests—perhaps particularly for the tensile test (in view of the various uncertainties associated with the flattening process).

4. FEM Modeling Outcomes

Outcomes of the FEM modeling are shown in **Figure 13** and **14**, which relate to pipes P1 and P2. The (true) stress–strain relationships used are based on the Voce parameter sets shown in **Table 2**, obtained from the PIP testing of these two steels.

Figure 13 shows the through-thickness distributions of residual stress and strain after flattening. These are from the central region; they do not incorporate the edge effects along the four edges of the sample, which occur only in relatively thin regions. As expected, the von Mises (equivalent plastic) strains peak at the inner and outer free surfaces, being slightly higher near the inner surface (negative distance from the neutral plane). They're both quite close to values of about 2% (P1) and 4% (P2), which correspond approximately to the h/R ratios for these pipes. The distributions of the individual strains are also of interest. The hoop strains are, as expected, approximately equal to $-\gamma/R$, where γ is the distance (in the radial direction) from the neutral plane. The axial strains, however, are low (limited by mutual constraint). Volume is being conserved (for plastic straining) by these hoop strains being balanced by the radial strains, ϵ_r , which are much less constrained than the axial strains and have a value of approximately $-\epsilon_\theta$.

There is a clear expectation that these prior plastic strains will harden the regions concerned during subsequent tensile testing, depending on the work hardening rate of the steel (higher for P2, see **Figure 7** and **8**). It's not, however, immediately clear what effect these prior strains, and also the residual stresses, will have

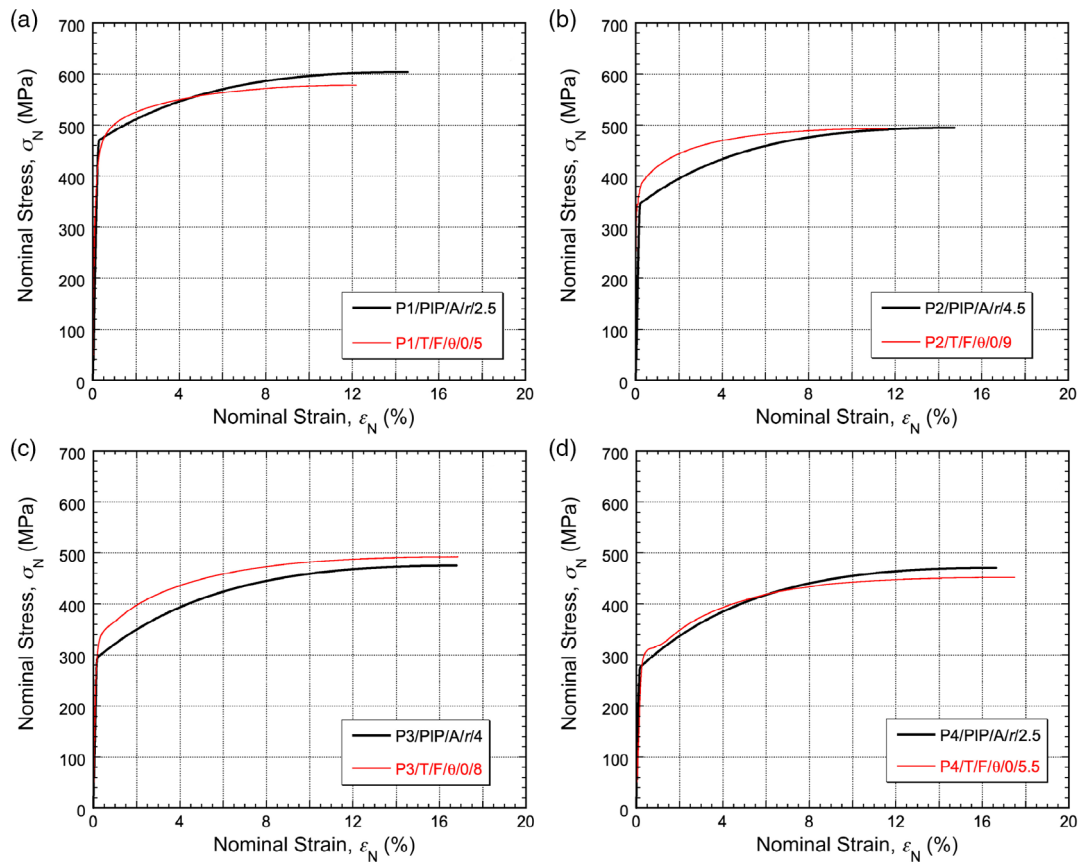


Figure 12. Comparisons between the stress–strain curves derived from PIP testing of the outer surface of as-received pipes and those obtained by hoop direction tensile testing of flattened pipes, for a) P1, b) P2, c) P3, and d) P4.

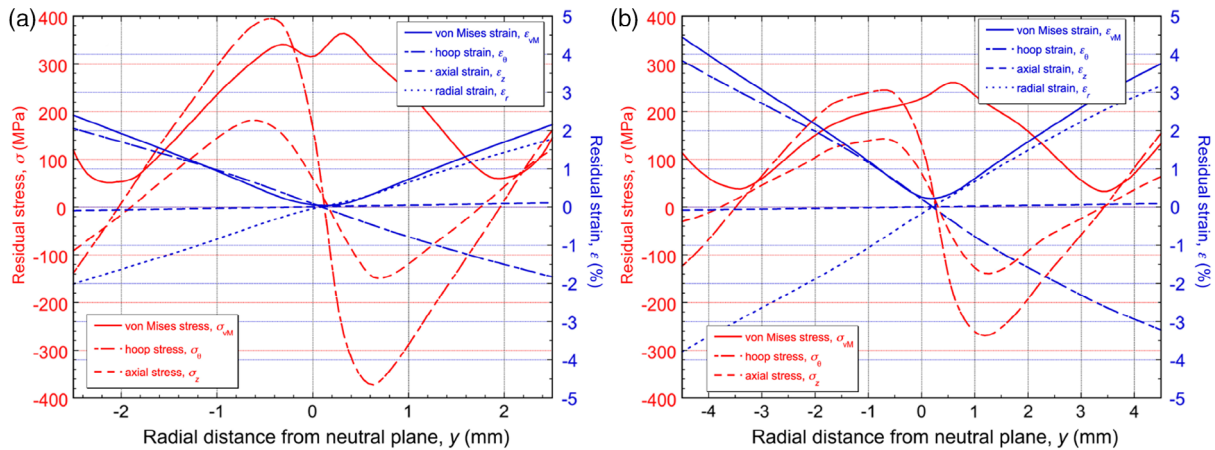


Figure 13. Predicted through-thickness distributions of residual stresses and strains after flattening for a) P1 and b) P2.

on the tensile response of the whole section. These residual stresses are higher for P1, reflecting the higher yield stress for that steel.

Predicted effects of these residual stresses and strains on tensile testing outcomes are shown in Figure 14. In both cases, there is significant hardening and also a slight tendency for the yielding to become more transitional (gradual). Similar effects are

observed for both pipes, although they are stronger for P2. This is a reflection both of the higher residual strains (higher h/R) for that pipe and of the higher work hardening rate for the steel. The residual stresses in the hoop direction are compressive in the upper (outer) half of the section and tensile in the lower (inner) half. These would be expected to respectively inhibit and promote yielding, although of course there is

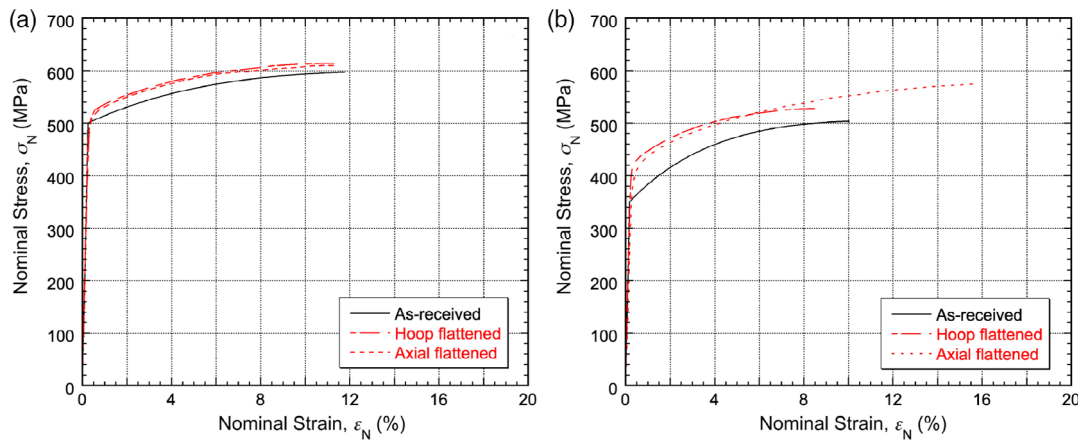


Figure 14. Predicted (nominal) stress–strain curves for tensile testing of complete wall sections, before and after flattening of a) P1 and b) P2.

Table 2. Sets of Voce parameter values used for FEM modeling of the flattening and subsequent (whole section) tensile response of two of the pipes.

Pipe Code	Yield stress, σ_y [MPa]	Saturation stress, σ_s [MPa]	Characteristic strain, ϵ_0 [%]
P1	500	750	10
P2	350	590	5

considerable overall constraint on the response of the complete section. It is likely, however, to be at least partly responsible for the more transient nature of the initial yielding. Both hoop and axial directions are similarly hardened, presumably because it's mainly the prior von Mises strains that are dictating the hardening; these are the same for testing in either direction.

In terms of comparing these outcomes with the experimental results, there is certainly broad consistency. Tensile hoop and axial curves for the flattened samples are similar in all cases. Moreover, Figure 3a, 4a, 5a, and 6a show that, in general, the flattened (red) curves tend to be a little harder, and perhaps a little more transient, than the as-received (black) curves, although the latter refer to axial loading (since tensile testing cannot be done in the hoop direction on as-received pipe). There are also some complications in the form of the as-received material showing some inhomogeneity and, for two of the steels, from the strain bursting observed in the as-received state. Of course, the PIP testing cannot be used directly to obtain whole section responses, but those outcomes do provide evidence that the flattened material is often harder in the near-surface regions than in the center. This is confirmed by the results of the reduced section tensile tests, although it should be noted that the as-received pipe may also exhibit some such inhomogeneity.

5. Conclusion

The following conclusions can be drawn from this work, which involves study of effects of the flattening of pipe sections on subsequent tensile test outcomes, with the PIP technique being used

to obtain insights into the behavior. The work is based on detailed study of four pipes made of different plain carbon steels, of a type that is commonly used for long-distance transmission of oil and gas. They cover a range of stress–strain relationships and pipe wall thicknesses and, taken as a group, they are thought to be broadly representative of the pipelines in industrial use. 1) Tensile testing of both whole pipe sections and partial (near-surface and central) sections, before and after flattening, has revealed certain features. These include a tendency in some cases for the as-received pipe to be a little harder near the free surfaces (inner and outer) and for this effect to be slightly enhanced in flattened pipes. Whole section tests have indicated that the flattening tends to raise the stress–strain curve slightly. 2) PIP testing outcomes are broadly consistent with these reduced section tensile test results, although they reflect the behavior in thinner near-surface regions and hence tend to be more sensitive to such regions being harder than the interior. PIP testing has also revealed that these pipes exhibit little or no anisotropy, which simplifies the interpretation of results. 3) One of the objectives is to infer the whole section tensile stress–strain curve of a flattened pipe, tested in the hoop direction, from the PIP-derived stress–strain curve obtained on the outer surface of an as-received pipe. Since the outer surface of as-received pipes tends to be slightly harder than the interior, but the flattening operation often causes some hardening, these two effects tend to cancel out, such that the PIP-derived curve is quite close to the target tensile curve. It certainly doesn't appear to be appropriate to make any universal “corrections” to a PIP-derived curve. 4) FEM modeling has been used to obtain insights into the effect of flattening operations on the resultant residual stresses and strains and on the subsequent whole section tensile testing outcome. These results are broadly consistent with the observed behavior.

Acknowledgements

Financial support is acknowledged from EPSRC, via grant no. EP/I038691/1. Relevant support was received from the Leverhulme Trust, in the form of an International Network grant (IN-2016-004) and an Emeritus Fellowship (EM/2019-038/4). In addition, an ongoing Innovate UK grant (project

number 10006185) covered work in this area and J.E.C. is in receipt of a Future Leaders grant from Innovate UK (MR/W01338X/1), which is focused on PIP usage.

Conflict of Interest

The authors declare no conflict of interest.

Data Availability Statement

The data that support the findings of this study are available from the corresponding author upon reasonable request.

Keywords

finite-element method modeling, indentation plastometry, pipelines, tensile testing

Received: December 7, 2022

Revised: January 26, 2023

Published online:

-
- [1] T. W. Clyne, J. E. Campbell, *Testing of the Plastic Deformation of Metals*, Cambridge University Press, Cambridge, UK **2021**, <https://doi.org/10.1017/9781108943369>.
- [2] M. Z. Wang, J. J. Wu, Y. Hui, Z. K. Zhang, X. P. Zhan, R. C. Guo, *Mater. Sci. Eng., A* **2017**, *679*, 143.
- [3] Y. W. Hwang, K. P. Marimuthu, N. Kim, C. Lee, H. Lee, *Int. J. Mech. Sci.* **2021**, *197*, 106291.
- [4] M. Z. Wang, L. B. Gao, K. Cao, J. J. Wu, W. D. Wang, *Measurement* **2021**, *171*, 108812.
- [5] K. Jeong, K. Lee, S. Lee, S. G. Kang, J. Jung, H. Lee, N. Kwak, D. Kwon, H. N. Han, *Int. J. Plast.* **2022**, *157*, 103403.
- [6] T. W. Clyne, J. E. Campbell, M. Burley, J. Dean, *Adv. Eng. Mater.* **2021**, *23*, 21004037.
- [7] J. E. Campbell, H. Zhang, M. Burley, M. Gee, A. T. Fry, J. Dean, T. W. Clyne, *Adv. Eng. Mater.* **2021**, *23*, 2001496.
- [8] M. Burley, J. E. Campbell, R. Reiff-Musgrove, J. Dean, T. W. Clyne, *Adv. Eng. Mater.* **2021**, *23*, 2001478.
- [9] Y. T. Tang, J. E. Campbell, M. Burley, J. Dean, R. C. Reed, T. W. Clyne, *Materialia* **2021**, *15*, 101017.
- [10] W. Gu, J. E. Campbell, Y. T. Tang, H. Safaie, R. Johnston, Y. Gu, C. Pleydell-Pearce, M. Burley, J. Dean, T. W. Clyne, *Adv. Eng. Mater.* **2022**, *24*, 2101645.
- [11] J. E. Campbell, M. Gaiser-Porter, W. Gu, S. Ooi, M. Burley, J. Dean, T. W. Clyne, *Adv. Eng. Mater.* **2022**, *24*, 2101398.
- [12] L. E. Collins, M. Rashid, in *10th Int. Pipeline Conf.*, Calgary **2014**, <https://doi.org/10.1115/IPC2014-33684>.
- [13] M. Rashid, S. Chen, L. E. Collins, in *12th Int. Pipeline Conf. (IPC 2018)*, Calgary **2018**, <https://doi.org/10.1115/IPC2018-78311>.
- [14] S. Kang, J. G. Speer, C. J. Van Tyne, T. S. Weeks, *Metals* **2018**, *8*, 354.
- [15] P. Nayyar, D. Dimopoulos, W. Walsh, in *13th Int. Pipeline Conf.* **2021**, Virtual online, <https://doi.org/10.1115/IPC2020-9429>.
- [16] S. Neupane, S. Adeb, R. Cheng, J. Ferguson, M. Martens, *J. Appl. Mech.* **2012**, *79*, 051002.
- [17] B. Sener, M. E. Yurci, *J. Test. Eval.* **2018**, *46*, 2584.
- [18] S. Hao, X. H. Dong, *Modell. Simul. Mater. Sci. Eng.* **2020**, *28*, 055009.
- [19] A. Yonezu, K. Yoneda, H. Hirakata, M. Sakihara, K. Minoshima, *Mater. Sci. Eng., A* **2010**, *527*, 7646.
- [20] K. Komori, *Int. J. Mech. Sci.* **2005**, *47*, 1838.
- [21] M. Fernandes, N. Marouf, P. Montmitonnet, K. Mocellin, *ISIJ Int.* **2020**, *60*, 2917.
- [22] R. Reiff-Musgrove, W. Gu, J. E. Campbell, J. Reidy, A. Bose, A. Chitrapur, Y. T. Tang, M. Burley, T. W. Clyne, *Adv. Eng. Mater.* **2022**, *24*, 2200642.
- [23] Y. T. Tang, R. Reiff-Musgrove, W. Gu, J. E. Campbell, M. Burley, J. Dean, T. W. Clyne, *Mater. Sci. Eng., A* **2022**, *848*, 143429.